11, 167.
Chang, N., and Schmid, H. H. O. (1973), *Biochem. Biophys. Res. Commun. 54*, 648.
Chu, H. P. (1949), *J. Gen. Microbiol. 2*, 255.
Folch, J., Lees, M., and Sloane Stanley, G. H. (1957), *J. Biol. Chem. 226*, 497.
Hirt, R., and Berchtold, R. (1957), *Helv. Chim. Acta 40*, 1928.
Hirt, R., and Berchtold, R. (1958), *Pharm. Acta Helv. 33*, 349.
Kozhukov, V. I., Molotkovskii, Y. G., and Bergelson, L. D. (1969), *Izv. Akad. Nauk SSSR, Ser. Khim. 7*, 1559.
Lin, J. T., and Baumann, W. J. (1974), *Biochem. Biophys. Res. Commun. 59*, 100.
Mahadevan, V., Phillips, F., and Lundberg, W. O. (1966), *Lipids 1*, 183.
Molotkovskii, Y. G., Kozhukhov, V. I., and Bergelson, L. D. (1971), *Biokhimiya 36*, 934.
Ottolenghi, A. C. (1965), *Biochim. Biophys. Acta 106*, 510.
Reman, F. C., Demel, R. A., de Gier, J., van Deenen, L. L. M., Eibl, H., and Westphal, O. (1969), *Chem. Phys. Lipids 3*, 221.
Schmid, H. H. O., Jones, L. L., and Mangold, H. K. (1967), *J. Lipid Res. 8*, 692.
Schupp, E., and Baumann, W. J. (1973), *J. Lipid Res. 14*, 121.
Turner, D. L., Holburn, R. R., Silver, M. J., and Baczynski, E. (1972), *Lipids 7*, 680.
Vaver, V. A., Shchennikov, V. A., and Bergelson, L. D. (1967), *Biokhimiya 32*, 1027.

Phase Separations in Phospholipid Membranes†

Stephen Hong-wei Wu and Harden M. McConnell*

ABSTRACT: Phase diagrams representing lateral phase separations in the plane of lipid bilayer membranes have been determined for binary mixtures containing dielaidoylphosphatidylcholine together with dimyristoylphosphatidylcholine, dipalmitoylphosphatidylcholine, distearoylphosphatidylcholine, dioleoylphosphatidylcholine, and dipalmitoylphosphatidylethanolamine. The phase diagrams were deduced from observations of the temperature dependence of the paramagnetic resonance spectra of low concentrations of spin-labels incorporated in these bilayer membranes. In one case, the binary mixture of dipalmitoylphosphatidylethanolamine and dielaidoylphosphatidylcholine, evidence has been obtained for fluid–fluid immiscibility, in specified temperature and composition ranges. This immiscibility could give a lateral phase separation into fluid domains in the plane of the membrane, and/or a transverse phase separation into an asymmetrical bilayer membrane, and/or possibly discontinuous bilayer membranes of different composition. An asymmetrical bilayer membrane can be expected on theoretical grounds to form a nonplanar membrane.

A large number of experimental studies of thermally induced fluid ⇌ gel phase transitions in phospholipid bilayers have been carried out, using a variety of physical techniques. For leading references to the earlier literature, see Shimshick and McConnell (1973a,b). Theoretical (statistical mechanical) studies of these transitions have also been made (Nagle, 1973). Recently, Shimshick and McConnell (1973a,b) have used spin-labels to derive phase diagrams for a number of binary mixtures of lipids in excess water. These diagrams represent lateral phase separations of lipids into domains of differing composition and fluidity. For certain binary mixtures of phosphatidylcholines the sizes and proportions of fluid and solid domains can be visualized directly using freeze fracture electron microscopy; the relative proportions of fluid and solid domains can be accounted for by the phase diagrams obtained from paramagnetic resonance data (Grant *et al.*, 1974a). This visualization can be facilitated by the incorporation of certain intrinsic membrane proteins into the binary lipid mixtures, since some of these proteins associate preferentially with fluid (F) rather than solid (S) lipid domains[1] (Kleemann *et al.*, 1974; Grant and McConnell, 1974b; Chen and Hubbell, 1973).

Aside from their inherent interest, phase diagrams for binary lipid mixtures are of biophysical and biochemical interest for at least three reasons. (i) In special fatty acid auxotrophs of *Escherichia coli* the fatty acid composition of the membranes can approximate that of a binary mixture of lipids; lateral phase separations in these membranes can be detected using spin-labels, and freeze-fracture electron microscopy, and can be correlated with the temperature dependence of the rates of sugar uptake into these cells (Linden *et al.*, 1973; Kleemann and McConnell, 1974). (ii) In view of the marked effect of solid phase–fluid phase equilib-

† From the Stauffer Laboratory for Physical Chemistry, Stanford, California 94305. *Received September 12, 1974.* This research has been supported by the National Science Foundation under Grant No. GB 38654. It has benefited from facilities made available to Stanford University by the Advanced Research Projects Agency through the Center for Materials Research.

[1] Abbreviations used are: F-phase lipids, a pure lipid, or a mixture of lipids, in the "fluid" state where there is a relatively high rate of lateral diffusion, and a high binding affinity for small hydrophobic molecules; S-phase lipids, a pure lipid, or a mixture of lipids, in the "solid" state where there is a relatively low rate of lateral diffusion, and a low binding affinity for small hydrophobic molecules; Tempo, 2,2,6,6-tetramethylpiperidine-1-oxyl; DPPC, *O*-(1,2-dipalmitoyl-*sn*-glycero-3-phosphoryl)choline; DPPE, *O*-(1,2-dipalmitoyl-*sn*-glycero-3-phosphoryl)ethanolamine; DMPC, *O*-(1,2-dimyristoyl-*sn*-glycero-3-phosphoryl)choline; DSPC, *O*-(1,2-distearoyl-*sn*-glycero-3-phosphoryl)-choline; DEPC, *O*-(1,2-dielaidoyl-*sn*-glycero-3-phosphoryl)choline; DOPC, *O*-(1,2-dioleoyl-*sn*-glycero-3-phosphoryl)choline.

ria on membrane protein distributions, these equilibria must clearly be taken into consideration in membrane reconstitution experiments. (iii) Finally, it is likely that a study of the relation between membrane protein function and lipid composition may provide important clues as to the molecular events accompanying these functions.

In all previous studies of binary lipid mixtures, complete miscibility of the lipids in the fluid phase was observed, whereas in a number of cases only limited miscibility in the solid phase was observed. In view of the frequent occurrence of liquid–liquid immiscibility among common liquids (*e.g.*, water and carbon tetrachloride) we have undertaken a study, described below, of a number of new binary lipid mixtures to see if any of them would show fluid phase immiscibility, or other novel features in their phase diagrams. The potential biophysical significance of fluid phase immiscibility is discussed later in the present paper. For the present study, we chose dielaidoylphosphatidylcholine as one component of the binary mixtures. This choice was based on its ease of preparation and the fact that its chain melting temperature (the F ⇌ S transition temperature), 12°, is particularly convenient experimentally. Unfortunately, as discussed later, this phospholipid is not ideal in other respects.

Materials and Methods

Sample Preparation. Dimyristoylphosphatidylcholine (DMPC), dipalmitoylphosphatidylcholine (DPPC), distearoylphosphatidylcholine (DSPC), and dipalmitoylphosphatidylethanolamine (DPPE) were obtained from Calbiochem and were used without further purification. Impurity content for each lipid was about 1% as judged by thin-layer chromatography. All phospholipids used in the present work are believed to have a single configuration.

Dielaidoylphosphatidylcholine (DEPC) and dioleoylphosphatidylcholine (DOPC) were prepared by the method of Cubero Robles and van den Berg (1969) from *O*-(*sn*-glycero-3-phosphoryl)choline (available as the $CdCl_2$ adduct from Sigma), and the anhydrides and sodium salts of elaidic acid (Analabs) and oleic acid (Sigma). The products were purified by column chromatography on silica gel (Bio-Sil A 200–325 mesh) and eluted with a chloroform–methanol gradient. DEPC emerged at 35–40% methanol and gave a single spot on silica gel plates. However, DOPC emerged at 18–30% methanol and gave a major phosphatidylcholine spot and detectable impurity of fatty acid due to large excess of oleic acid and acid anhydride according to the above synthetic method. Crude DOPC was again purified on a second silica gel column eluted with chloroform–methanol. DOPC was collected at 20–25% methanol and gave only one spot on silica gel plates. Both DEPC and DOPC have the same R_F value as egg lecithin on thin-layer chromatograms developed in chloroform–methanol–water (65:24:4 v/v). Both products were stored as stock solutions in ethanol (under argon at −20°). Concentrations were determined by the method of McClare (1971).

Tempo was a gift of K. L. Wright. The spin-label, formula II, was prepared by acylation of pure DPPC lysolecithin with the spin-label fatty acid anhydride, as described by Hubbell and McConnell (1971) and was a gift of Dr. C. W. M. Grant in this laboratory.

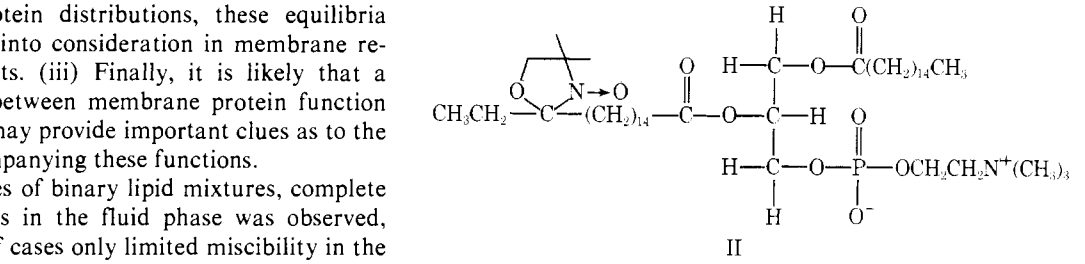

II

Phospholipid Dispersions. The desired binary mixtures of lipids were mixed in chloroform–ethanol solution and coated on the inside of 10-ml flasks by removal of the solvent under vacuum. Each 35–40-μmol sample was resuspended in 200–250 μl of 0.01 M sodium phosphate buffer (pH 7.0) by vortexing at a temperature higher than the upper transition temperature of the two lipids; 75 μl of a 2 mM Tempo solution was then added and a portion of the lipid dispersion was transferred to a 50-μl capillary pipet used as a sample cell for electron paramagnetic resonance (epr) measurement. The final lipid concentration was about 8–11% by weight. This is close to the concentration range used by Shimshick and McConnell (1973a).

When II was used in experiments for constructing phase diagrams for DEPC–DPPE and DOPC–DPPE systems, 25–30 μl of a 6.17 mM ethanolic solution of II was added directly to a $CHCl_3$/EtOH solution containing 20–25 μmol of a binary lipid mixture. Only about 0.5–1 mol % of the total lipid was label II. The solvent was then removed under vacuum as described above for the Tempo experiments; 150–200 μl of 0.01 M sodium phosphate buffer at pH 7.0 was added to the dried sample to keep the final lipid concentration approximately about 8–11% by weight.

Each sample flask was shaken vigorously on a vortex mixer for 10 min, and the temperature during agitation was kept slightly above 65° (the transition temperature of DPPE). A portion of the lipid suspension was sealed in a 50-μl pipet under argon. The sample cells for the Tempo and the label II experiments prepared by this method gave good reproducible results within a reasonable period of time (at least 1 or 2 weeks), whenever back checks were necessary.

Paramagnetic Resonance Spectroscopy. Quantitative measurements with spin-labels require reproducible sample insertion and accurate temperature control. Detailed descriptions of the sample cell holder and temperature control accessories are given elsewhere (McFarland, 1974).

In brief, both the Tempo spectral parameter, f, and the high field signal height of the label II spectrum, H_h, were measured as a function of temperature. All measurements were made on a Varian E-12 spectrometer operating at X-band with the sample in a horizontal position to minimize the settling of the phospholipid liposomes in the sample tube. The temperature was measured with a copper–constantan thermocouple connected to a Smith-Florence potentiometric microvoltmeter. Measurements were made both heating and cooling the sample at rates of 8–10°/hr. The Tempo spectral parameter is approximately equal to the fraction of molecules of Tempo dissolved in the fluid hydrophobic region of the membrane. In order to get comparable results for H_h the settings for the field (3250 G), modula-

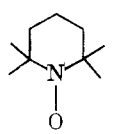

Tempo (I)

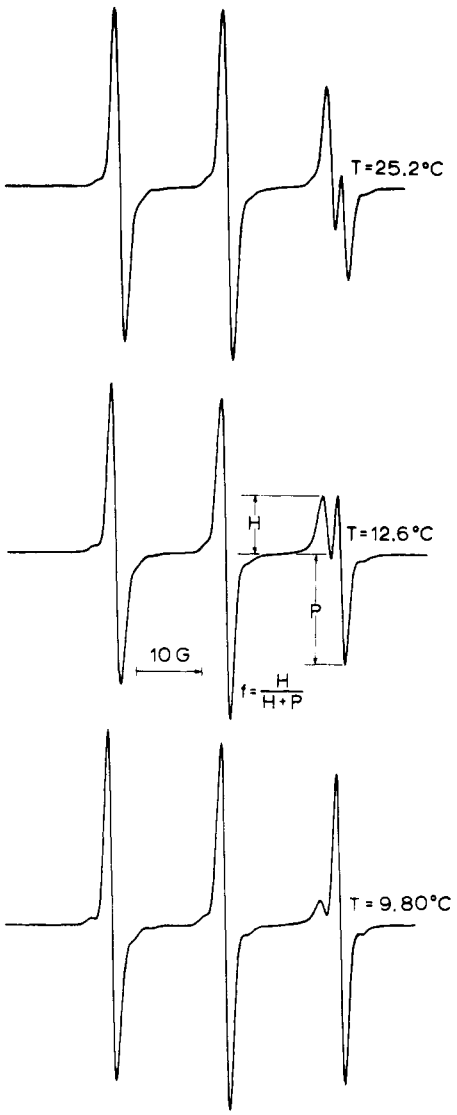

FIGURE 1: Paramagnetic resonance spectra of Tempo dissolved in aqueous dispersions of dielaidoylphosphatidylcholine (121 mg/ml) above, in the middle, and below the chain melting transition temperature (~12°).

tion amplitude (0.32 G), microwave power (5 mW), microwave frequency (~9.12 GHz), and detector current (250 μA) were all kept constant.

Results

Phase Transition of Dielaidoylphosphatidylcholine (DEPC). In Figure 1 are illustrated first derivative paramagnetic resonance spectra of Tempo in an aqueous dispersion of DEPC at three temperatures (above, in the middle, and below the phase transition).

Tempo dissolves readily in water and in the fluid (F) lamellar smectic liquid-crystalline phase of lipid bilayers (highly mobile hydrophobic acyl chains) but is largely excluded from solid (S), gel-phase (lipid acyl chains rigidly extended) (Shimshick and McConnell, 1973a; Kleemann *et al.*, 1974). Thus Tempo can be used to monitor this change in partition between aqueous and fluid lipid regions.

Since the hyperfine and *g*-tensors of the epr spectrum depend on the polarity of the spin-label environment, the high field spectral line can be partially resolved into two signals; one is due to Tempo in the fluid lipid region (indicated as H in Figure 1) and the other is due to Tempo in the aqueous

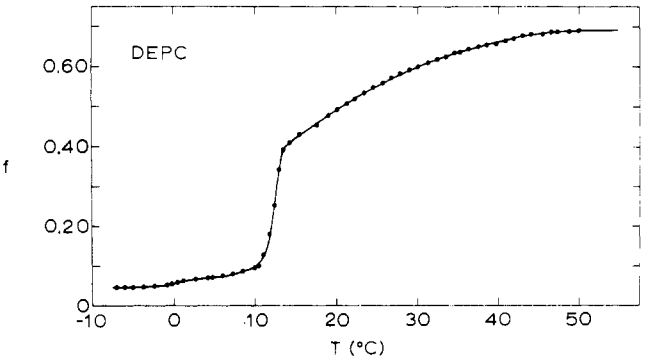

FIGURE 2: The Tempo spectral parameter, *f*, *vs.* temperature for an aqueous dispersion of DEPC (121 mg/ml); see text.

region (P in Figure 1) (Shimshick and McConnell, 1973a; Kleemann *et al.*, 1974; Hubbell and McConnell, 1968). Experimentally, this permits one to measure a Tempo spectral parameter, *f*, equal to H/(H + P); which is approximately equal to the fraction of Tempo dissolved in the fluid lipid phase of the sample at any one temperature. (This parameter obviously depends on the concentration of the lipids in the aqueous dispersion. In the present work this concentration is typically 8–11% by weight, which is approximately the same as that used by Shimshick and McConnell (1973a,b). Therefore the values of *f* reported here can be compared directly with the earlier values of *f*, at least approximately.) Below the transition temperature where the pure lipid bilayers are in the solid (S) phase, the value of *f* is small; above the transition temperature where the lipid bilayers are in the F phase, the value of *f* is large. Thus, a plot of *f* vs. *T*, or $1/T$, for aqueous dispersions of pure phospholipids can be used to determine the transition temperature.

Shimshick and McConnell (1973a) have used this technique to measure transition temperatures for a number of saturated phospholipids. Here, we have applied the same technique to measure the transition temperature of pure DEPC dispersed in excess aqueous buffer. A plot of the Tempo spectral parameter, *f*, as a function of temperature for DEPC is illustrated in Figure 2. DEPC with an acyl chain length of 18 carbon atoms and a trans-9 double bound has a transition temperature 12°, defined as the average value of the beginning and the completion temperatures of the Tempo transition curve (10.5–13.5°). As discussed later, the phospholipid DEPC does appear to be somewhat unusual in that, as seen in Figure 2, the Tempo binding is strongly temperature dependent above the chain melting transition temperature.

Wu and McConnell (1973) have also used the electrical resistance of lipids impregnated in a fritted glass filter to determine transition temperatures. Using this technique we observed an abrupt change in membrane electrical conductivity between 12 and 14°, a result in agreement with the Tempo experiment.

The determination of the transition temperature of an aqueous dispersion of DOPC by the spin-label technique was not attempted due to its highly fluid nature below 0°. Phillips *et al.* (1970) estimated the transition temperature of DOPC by the technique of differential scanning calorimetry and reported that DOPC gave a large endothermic transition about −22°. We use this temperature of DOPC in our later discussion.

Phase Separations and Phase Diagrams. Unlike single component phospholipid dispersions, binary mixtures of lip-

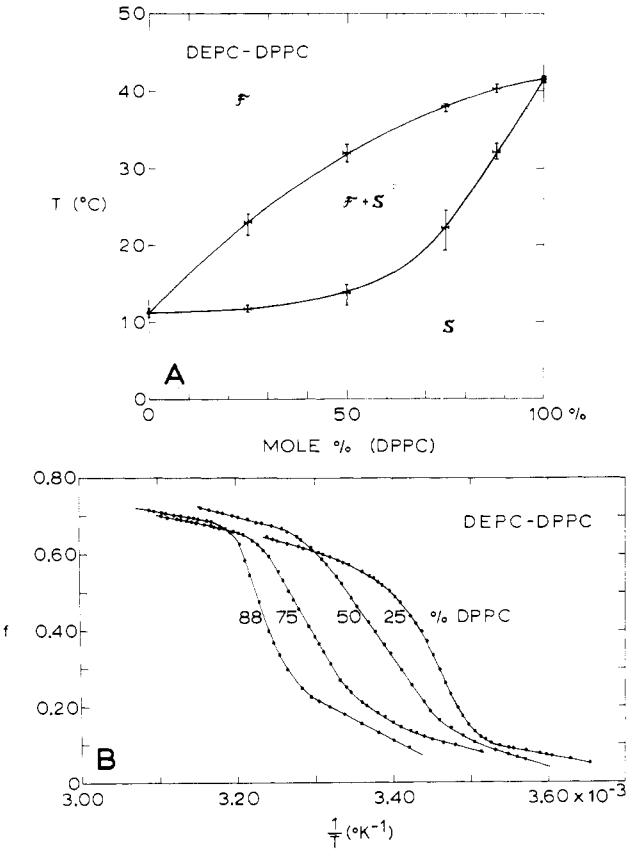

FIGURE 3: (A) Phase diagram for aqueous dispersions of the DEPC–DPPC binary system; temperature *vs.* mole per cent DPPC. Regions of the phase diagram containing fluid (F) phase only, solid phase (S) only, and an equilibrium mixture of solid and fluid (S + F) phases are shown. (B) Experimental Tempo spectral parameter, f, as a function of $1/T$ for 88, 75, 50, and 25 mol % DPPC.

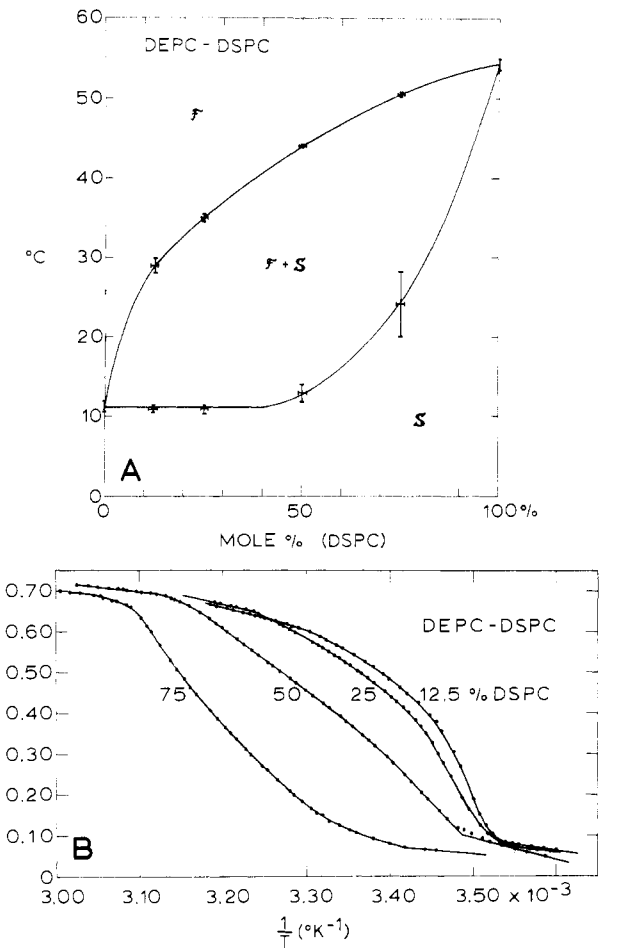

FIGURE 4: (A) Phase diagram for aqueous dispersions of the DEPC–DSPC binary system. (B) Experimental Tempo spectral parameter, f, as a function of $1/T$ for 75, 50, 25, and 12.5 mol % DSPC.

ids in excess buffer do not usually exhibit a sharp transition temperature (Shimshick and McConnell, 1973a; Shimshick *et al.*, 1973; Kleemann *et al.*, 1974). Instead, two characteristic temperatures, T_f and T_s, are found from the plots of the Tempo spectral parameter, f, as a function of reciprocal temperature, $1/T$, as shown in Figures 3B, 4B, and 5B. The higher temperature break, T_f, and the lower break, T_s, are interpreted to signify that all lipids are in the F state above T_f, and are in the S state below T_s. Between those two characteristic temperatures, domains of F phase and S phase are simultaneously present in the bilayers.

According to the studies of Shimshick and McConnell (1973a), these results (curves of f *vs.* $1/T$) can be interpreted in terms of phase diagrams that describe two-dimensional equilibria between F and S phases, with different phospholipid compositions for each phase. Plots of higher temperature breaks, T_f's, *vs.* various corresponding compositions of binary lipid mixtures define the upper (*fluidus*) curve in a phase diagram. Similarly, lower temperature breaks, T_s's, and the corresponding lipid mixture compositions define the lower (*solidus*) curve in the same phase diagram. In the systems of binary *saturated* lipids studied by Shimshick and McConnell (1973a) two general types of phase diagrams were found, namely, solid solution–fluid solution and partial miscibility in the solid phase.

The plots of f *vs.* $1/T$ for the F–F and S–S solutions show a gradual decrease of f over the entire temperature range. These curves look like broadened transition curves. The *solidus* and *fluidus* boundaries in the phase diagrams are continuous curves without discontinuities in slope. For the phase diagrams with partially immiscible S phases, the Tempo spectral parameter curves typically exhibit three relatively abrupt changes in slope and their shapes depend on the relative amounts of each lipid in the mixture. This type of phase diagram has two features: a discontinuity in the slope of the solidus curve together with a theoretically expected intersection of a third line at this point of discontinuity (which is not easily detectable using Tempo) and a horizontal solidus line. In this case, the lipids have a limited S-phase miscibility, and two solid phases coexist as heterogeneous mixtures over a certain range of compositions.

Binary mixtures of DEPC and DPPC exhibit Tempo spectral parameter–temperature curves (Figure 3B) with quite distinct high and low temperature breaks. The two (high and low) characteristic temperatures are determined by the intersections of straight lines which are drawn through the three distinct regions in each curve. The phase diagram derived from these characteristic temperatures and the corresponding lipid compositions is illustrated in Figure 3A. This phase diagram falls in the category of solid-solution and fluid-solution type in which the lipids form a complete range of F and S phase solutions.

Binary mixtures of DEPC and DSPC have Tempo spectral parameter curves and the phase diagram given in Figure 4A and B. In some of the curves shown in Figure 4B (12.5, 25, and 50 mol % DSPC), it is clearly seen that there are three relatively abrupt changes in slope for each curve.

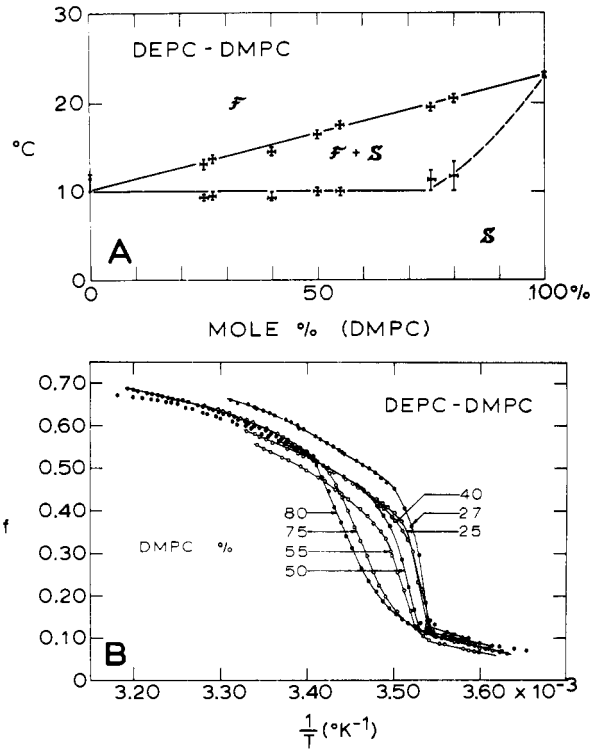

FIGURE 5: (A) Phase diagram for aqueous dispersions of the DEPC–DMPC binary system. (B) Experimental Tempo spectral parameter, f, as a function of $1/T$ for 80, 75, 55, 50, 40, 27, and 25 mol % DMPC.

These curves, particularly at low DSPC concentrations, give rapid drops in f on the plots of f *vs.* $1/T$. Thus, the phase diagram indicates the DEPC and DSPC mixtures do not form a complete range of solid phase solutions but rather have a limited solid phase miscibility.

Binary mixtures of DEPC–DMPC show the Tempo spectral parameter curves in Figure 5B and the phase diagram in Figure 5A. It is interesting to see that data points for the fluidus curve in the phase diagram fall in a straight line defined by the transition temperatures of DEPC and DMPC. The horizontal line of the solidus curve almost covers the entire range of compositions (up to ~80 mol % DMPC). This phase diagram approaches the limiting case of complete S-phase immiscibility.

Binary mixtures of DEPC–DPPE show the Tempo spectral parameter curves in Figure 6B. For lipid compositions up to about 70 mol % DPPE, the plots of f *vs.* $1/T$ show the same temperature as the transition temperature of DEPC for the lower characteristic temperature breaks. The solidus curve in the phase diagram given in Figure 6A is thus a distinct horizontal line having a presumed discontinuity in slope at about 70 mol % DPPE. It indicates S-phase immiscibility up to this composition and solid solutions beyond this composition. A second discontinuity in slope of the solidus curve was also found at 85 mol % DPPE.

It is extremely interesting to see that there are two distinct features about the curve drawn from the higher characteristic temperature breaks of Tempo spectral parameter curves. (a) The higher temperature breaks for lipid compositions of ~10 mol % to ~50 mol % DPPE are all approximately equal, about 50°, and thus give a horizontal line in the phase diagram. (b) There is a slope discontinuity at about 50 mol % DPPE.

In order to verify the presence of the horizontal line, the second label, label II, was used. The results are shown in

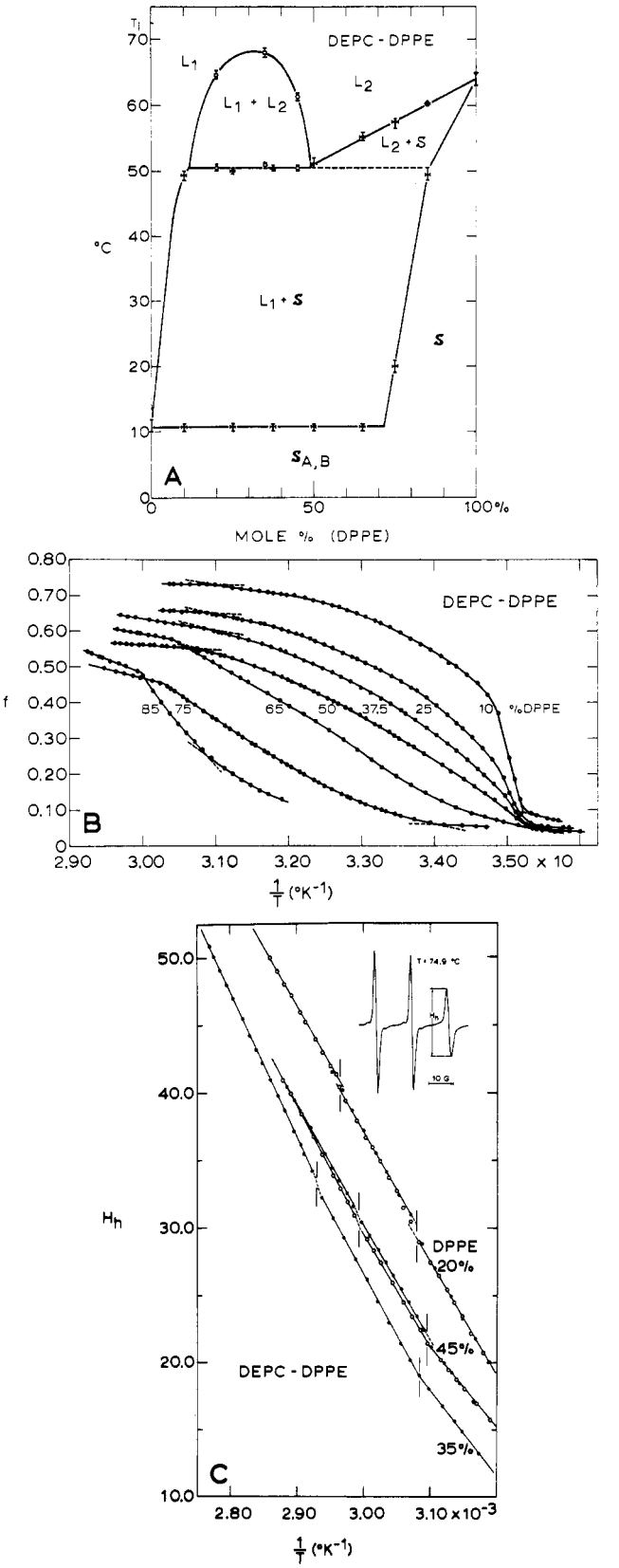

FIGURE 6: (A) Phase diagram for aqueous dispersions of the DEPC–DPPE binary system. (⊕) Data taken from temperature breaks of experimental Tempo spectral parameter curves in Figure 6B; (⊖) data taken from temperature breaks of H_h *vs.* $1/T$ in Figure 6C. (B) Experimental Tempo spectral parameter, f, as a function of $1/T$ for 85, 75, 65, 50, 37.5, 25, and 10 mol % DPPE. (C) High field signal height, H_h (in arbitrary units), of the phospholipid spin-label II (less than 1 mol % in total lipid (see text) as a function of temperature for 20, 35, and 45 mol % DPPE aqueous dispersions. (●) Cooling curve; (○) heating curve.

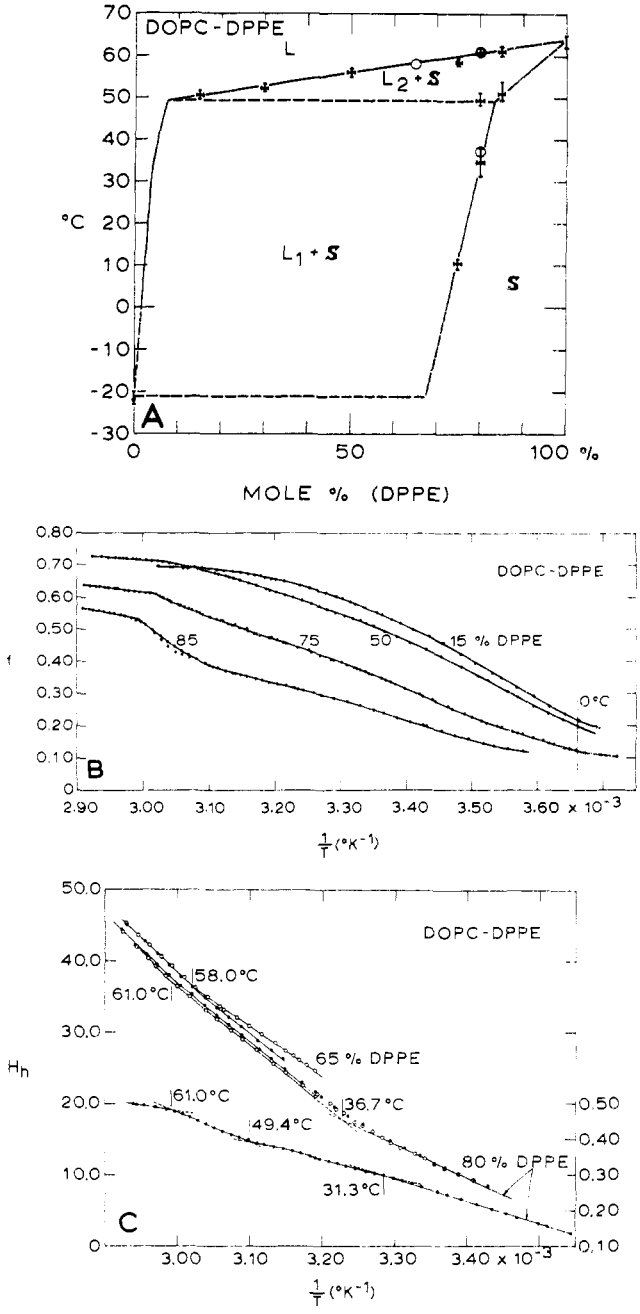

FIGURE 7: (A) Phase diagram for aqueous dispersions of the DOPC-DPPE binary systems. (⊕) Data taken from temperature breaks in experimental Tempo spectral parameter curves in Figure 7B; (○) data taken from temperature breaks of H_h *vs.* $1/T$ in Figure 7C. (B) Experimental Tempo spectral parameter, f, as a function of $1/T$ for 85, 75, 50, and 15 mol % DPPE. (C) Upper curves: High field signal height, H_h (in arbitrary unit), of II (less than 1 mol % in total lipid) as a function of $1/T$ for aqueous dispersions of 65 and 80 mol % DPPE. (○) Heating curve; (●) cooling curve. Experimental Tempo spectral parameter, f, as a function of $1/T$ for 80 mol % DPPE is shown in lowest curve of Figure 7C.

Figure 6C. The paramagnetic resonance spectrum of label II in a binary mixture of 35 mol % DPPE is given in the upper part of Figure 6C. The plots of the high field signal height, H_h, in arbitrary units, as a function of reciprocal temperature for three aqueous lipid dispersions with compositions between 10 and 50 mol % DPPE are given in Figure 6C. Each curve exhibits two breaks shown as a discontinuity in the curve, or as an abrupt change in slope of the curve. Although these curves were not always quantitatively reversible, the qualitative observation of two temperature breaks is reproducible.

The lower breaks (designated as T_l*) for the above three mixtures have the same temperature ~51° as the higher characteristic temperature determined by the Tempo spectral parameter curves for compositions between 10 and 50 mol % DPPE. Thus there is little doubt that there is a horizontal line in the phase diagram in Figure 6A.

The highest temperature breaks in Figure 6C form a closed region with a horizontal base line as given above. This can be interpreted as defining an area of limited F-phase miscibility. Within this region, there are two mutually immiscible fluids, L_1 and L_2, with different compositions.

Shimshick and McConnell (1973a) have reported that the transition temperature of DPPC remains unchanged for DPPC to Tempo mole ratios of 400–800. Similarly, the concentrations of spin-label II, 0.05–1 mol % in total lipid concentrations, are sufficiently small that the label itself does not appreciably disturb the characteristic temperatures at which phase separations of the major lipids take place. This is observed from the excellent agreement of within 1° between those temperatures determined by both label II and Tempo. As expected, the L_1-L_2 immiscibility curve determined using the label II could not be detected using Tempo, because f depends primarily on the fraction of lipids in the fluid state. The sensitivity of the spectrum of the label II to L_1-L_2 phase separations probably has its origin in a small difference in the hyperfine splittings (or order parameters) in the two fluid phases. This small difference should affect the apparent line width of the high-field signal, and thus the apparent peak height.

Studies of Tempo binding at concentrations of DPPE above 50% and below 85% did not reveal any features clearly associated with the dotted horizontal line at ~51°. This is somewhat unexpected since on reducing the temperature below this dotted line the fraction of the lipids in the fluid phase should decrease significantly, and thus bring about a substantial reduction in the Tempo solubility. This expected decrease in Tempo solubility is nearly compensated for by another effect, the decrease in the proportion of DEPC in the fluid phase. As discussed later, DEPC has an unusually large temperature dependence of Tempo solubility above its chain melting transition temperature. As can be seen in Figure 2, f is about 0.7 for DEPC at 50°. From the work of Shimshick and McConnell (1973a), f is found for DPPE to be ~0.1 at 50° and only ~0.3 at 65° (the transition temperature of DPPE). A more detailed analysis is given below.

We adopt the quantitative analysis described by Shimshick and McConnell (1973a). The partition coefficients can be derived from the spectral parameter–temperature plots for the pure phospholipids above and below their transition temperatures. These partition coefficients can be represented by the empirical equation $K = c - (d/T)$, where c and d are constants. The partition coefficients for the pure lipids in the F phase are: DEPC, $K_F = 157 - (42{,}500/T)$ and DPPE, $K_F = 80 - (25{,}400/T)$, assuming that the volume ratio of the lipid regions to the aqueous regions is approximately equal to the weight ratio of the lipids in the aqueous dispersions. At 50°, K_F for DEPC is about 25 times higher than K_F of DPPE. Since the Tempo solubility in the S phase is effectively eliminated by the addition of small amounts of the phosphatidylethanolamine, the S-phase partition coefficient for each of the pure components in such binary mixtures can be assumed to be a small number (which was chosen as 0.7 by Shimshick and McConnell

(1973a) to fit the experimental minimum values of f). Thus, the approximate values of f can be calculated from K_F's and K_S (taken to be 0.7) and the fraction of the lipids in the F phase, F_F, from the phase diagram (Shimshick and McConnell, 1973a)

$$f = \frac{[K_F F_F + K_s(1 - F_F)]V_h/V_p}{1 + [K_F F_F + K_s(1 - F_F)]V_h/V_p} \quad (1)$$

where

$$K_F = (1 - X_F)(K_F)_{DEPC} + X_F(K_F)_{DPPE}$$

For any lipid compositions from 50 to 85 mol % DPPE in the binary system of DEPC and DPPE, the values of f calculated from eq 1 are about the same for the temperatures just slightly above and below 50° (*e.g.*, ~0.18 *vs.* 0.17 for 80 mol % DPPE, ~0.27 *vs.* 0.25 for 75 mol % DPPE). Thus the enrichment of DEPC in F phase below the monotectic temperature overcomes the abrupt drop of F_F, indicated from the phase diagram, such that the Tempo spectral parameter curves still show a gradual decrease in f without any abrupt break at the monotectic temperature.

Binary mixtures of DOPC–DPPE show the Tempo spectral parameter curves in Figure 7B. The higher characteristic temperatures, T_f's, determined from the plots of f *vs.* $1/T$ give a straight fluidus line in Figure 7A. The measurements of the lower characteristic temperatures below 0° were not attempted for any mixture due to the freezing of water in the system.

The *fluidus* curve is further examined by using II in lipid dispersions. The results are given in Figure 7C for 65 and 80 mol % DPPE. Each curve in Figure 7C is fully reversible within experimental errors. The breaks at higher temperature (Figure 7C) in the plots of H_h *vs.* $1/T$ fall on the straight fluidus line defined by the Tempo spectral parameter curves.

In order to determine the solidus curve, which is more ambiguous in this system, it is quite helpful to examine both plots of f *vs.* $1/T$ and H_h *vs.* $1/T$ for 80 mol % DPPE both in Figure 7C. Both curves show a broad and gradual, but detectable change in slope in a temperature range between 31 and 38°. This broad range of temperatures fits the solidus curve defined by the lower characteristic temperatures for 75 and 85 mol % DPPE quite well. Both 80 and 85 mol % DPPE exhibit clear breaks at about 50°, and a broad but still detectable change in 75 mol % DPPE at the same temperature in the Tempo spectral parameter curves. Since the fluidus curve exhibits a discontinuity at 85 mol % DPPE, it is reasonable to draw a horizontal line in Figure 7A through the compositions which show breaks at 50° to meet the fluidus curve.

Discussion

Of the five new phase diagrams reported in the present paper, only one represents fluid-fluid (F-F) immiscibility. The other four diagrams will not be discussed in detail here, since these types of diagrams have been discussed previously. However, two points may be noted. (a) The DEPC–DPPC diagram in Figure 3A has been shown elsewhere (Grant *et al.*, 1974a) to account for freeze-fracture electron microphotographs of bilayers that contain this pair of lipids. In other words, the diagram predicts the relative proportion of F and S domains that coexist at equilibrium. These domains can be seen with the electron microscope and are found to have the relative proportions predicted by the phase diagram in Figure 3A. (b) Three of the phase diagrams show clear regions of limited solid phase miscibility. Solid phase immiscibility is typical of pairs of lipids having sufficiently different physical properties, *viz.*, chain melting temperatures. These diagrams are qualitatively similar to those that apply to binary mixtures in which one component is a phosphatidylcholine, and the second component is cholesterol (Shimshick and McConnell, 1973b).

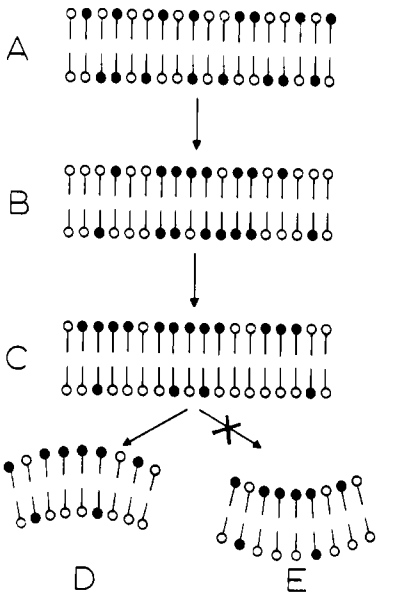

FIGURE 8: Schematic representation of possible consequences of limited fluid-fluid immiscibility of phospholipids. (A) Homogeneous fluid solution of black and white lipids. (B) Partial fluid-fluid immiscibility arising from lateral phase separation into regions relatively rich in white lipids, and regions rich in black lipids. (C) Transverse phase separations so that one-half of the bilayer is rich in black lipids and the other half is rich in white lipids. (D and E) Stable and unstable polarized distortion of membrane from a planar shape due to asymmetrical transverse distribution of lipids.

The phase diagram for the binary mixture of DEPC and DPPE is unique and represents to our knowledge the first evidence of F–F immiscibility. (Lateral phase separations in binary mixtures of phospholipids induced by Ca^{2+} have been reported by Ohnishi and Ito (1973) and may represent a special type of F–F immiscibility.) A thermodynamically stable spontaneous segregation of lipids into immiscible fluid domains is of obvious potential biophysical significance; however, the diagram in Figure 6A is of a limited immediate significance in this regard since DEPC is not a naturally occurring lipid, and the temperature region of F–F immiscibility is not typical of physiological temperatures. On the other hand, we have no reason to suspect that naturally occurring lipid mixtures will not show this F–F immiscibility at physiological temperatures.

One of the most interesting features of F–F immiscibility is the strong likelihood that this immiscibility will lead to (a) *an asymmetrical bilayer membrane*, and (b) *a polarized bilayer membrane*.

An asymmetrical bilayer membrane is created by placing F lipids of one composition on one side of the membrane, and by placing F lipids of the second composition on the other side, as indicated schematically in Figure 8. In a large, planar bilayer membrane, it is likely that this process is nearly neutral energetically (nearly zero free energy change). A chemically asymmetrical planar membrane will almost certainly lower its free energy by undergoing a distortion from a strictly planar shape, as indicated schematically in Figure 8. The following argument makes this idea

clear. Consider the two distortions, a convex distortion δ and a concave distortion $\delta' = -\delta$. The elastic restoring forces for these distortions are Force $= -k\delta$; Force$' = -k'\delta'$. Because of the physical asymmetry of the bilayer, these forces cannot be equal in magnitude when $\delta = -\delta'$. That is, for physical reasons, $k \neq k'$. Thus, the planar conformation cannot be the conformation of lowest energy. The simplest distortion to consider is one that gives rise to a simple, closed vesicle having a convex (bending outward) surface everywhere. In this case, the above argument leads to the idea that the membrane of this vesicle must be *polarized;* that is, there must be a preference for one lipid composition to face outwards, and for the second lipid composition to face inwards. Of course more complex distortions are possible. A biconcave disk having a shape analogous to the erythrocyte is an example. Here different regions of the same bilayer membrane should have opposite chemical polarizations.

The above ideas are related to, but are distinct from, the observation that small vesicles obtained by the strong sonication of binary mixtures of phospholipids have asymmetrical distributions of lipid composition (Michaelson *et al.*, 1973; Litman, 1974). Even when prepared from a single lipid these small, highly strained vesicles have lipids with distinguishable physical properties on the inside and outside (*e.g.*, difference in packing density). Thus, a difference in lipid composition in a binary mixture in a small vesicle produced by sonication is not totally surprising. Our discussion above concerning membrane asymmetry and polarization refers to states of thermodynamic equilibrium, in contrast to the sonicated vesicle experiments.

From the present work we cannot rigorously exclude the possibility that the phase separations actually result in noncontiguous lipid bilayers with different fluidity and composition, except on the grounds that the rates of fusion and fission of lipid vesicles are normally quite low. The study of Grant *et al.* (1974a) provides clear evidence that fission does not remove coexisting fluid and solid domains in single DEPC–DPPE bilayer membranes.

In spite of its convenient chain melting temperature (12°) we consider in retrospect that our choice of DEPC as the second component of the various binary lipid mixtures may have been unfortunate. This is because the large temperature dependence of Tempo solubility in this phospholipid *above* its transition temperature makes it sometimes difficult to discern the onset temperatures for lateral phase separations when the second component melts well above 12°. This is particularly true in the case of the important phase diagram in Figure 6A, where the large temperature dependence of the solubility of Tempo in DEPC itself well above its transition temperatures gives rise to some uncertainty in the analysis of the binding of Tempo to DEPC–DPPE mixtures. However, these uncertainties do not affect our conclusion that this pair of lipids does exhibit F–F immiscibility. The strong temperature dependence of the solubility of Tempo in DEPC above its chain melting temperature is of some interest in itself. In a sense, at high temperatures (>12°) the shape of the Tempo binding curve "anticipates" the chain-melting transition at lower temperatures. This may be due to the formation of small clusters of relatively ordered DEPC molecules above the chain-melting transition temperature (Lee *et. al.*, 1974) or, more probably, to a general and gradual increase in chain ordering throughout the lipid bilayer.

References

Chen, Y. S., and Hubbell, W. L. (1973), *Exp. Eye Res. 17,* 517.

Cubero Robles, E., and van den Berg, D. (1969), *Biochim. Biophys. Acta 187,* 52.

Grant, C. W. M., Wu, S. H. W., and McConnell, H. M. (1974a), *Biochim. Biophys. Acta 363,* 151.

Grant, C. W. M., and McConnell, H. M. (1974b), *Proc. Nat. Acad. Sci. U.S. 71,* 4653.

Hubbell, W. L., and McConnell, H. M. (1971), *J. Amer. Chem. Soc. 93,* 314.

Hubbell, W. L., and McConnell, H. M. (1968), *Proc. Nat. Acad. Sci. U.S. 61,* 12.

Kleemann, W., and McConnell, H. M. (1974), *Biochim. Biophys. Acta 345,* 220.

Kleemann, W., Grant, C. W. M., and McConnell, H. M. (1974), *J. Supra. Struct.* (in press).

Lee, A. G., Birdsall, N. J. M., Metcalf, J. C., Toon, P. A., and Warren, G. B. (1974), *Biochemistry 13,* 3699.

Linden, C., Wright, K., McConnell, H. M., and Fox, C. F. (1973), *Proc. Nat. Acad. Sci. U.S. 70,* 2271.

Litman, B. J. (1974), *Biochemistry 13,* 2844.

McClare, C. W. F. (1971), *Anal. Biochem. 39,* 527.

McFarland, B. G. (1974), *Methods Enzymol.* (in press).

Michaelson, D. M., Horwitz, A. F., and Klein, M. P. (1973), *Biochemistry 12,* 2637.

Nagle, J. F. (1973), *J. Chem. Phys. 58,* 252.

Ohnishi, S., and Ito, T. (1973), *Biochem. Biophys. Res. Commun. 51,* 132.

Phillips, M. C., Ladbrooke, B. D., and Chapman, D. (1970), *Biochim. Biophys. Acta 196,* 35.

Shimshick, E. J., and McConnell, H. M. (1973a), *Biochemistry 12,* 2351.

Shimshick, E. J., and McConnell, H. M. (1973b), *Biochem. Biophys. Res. Commun. 53,* 446.

Shimshick, E. J., Kleemann, W., Hubbell, W. L., and McConnell, H. M. (1973), *J. Supra. Struct. 1,* 285.

Wu, S. H. W., and McConnell, H. M. (1973), *Biochem. Biophys. Res. Commun. 55,* 484.